
Enhancing Transformation-based Defenses using a Distribution Classifier

Connie Kou

School of Computing, National University of Singapore
 Bioinformatics Institute, A*STAR Singapore
 koukl@comp.nus.edu.sg

Hwee Kuan Lee

School of Computing, National University of Singapore
 Bioinformatics Institute, A*STAR Singapore
 leehk@bii.a-star.edu.sg

Teck Khim Ng

School of Computing, National University of Singapore
 ngtk@comp.nus.edu.sg

Ee-Chien Chang

School of Computing, National University of Singapore
 changec@comp.nus.edu.sg

Abstract

Adversarial attacks on convolutional neural networks (CNN) have gained significant attention and research efforts have focused on defense methods that make the classifiers more robust. Stochastic input transformation methods have been proposed, where the idea is to randomly transform the input images to try to recover from the adversarial attacks. While these transformation-based methods have shown considerable success at recovering from adversarial images, the performance on clean images deteriorates as the magnitude of the transformation increases. In this paper, we propose a defense mechanism that can be integrated with existing transformation-based defenses and reduce the deterioration of performance on clean images. Exploiting the fact that the transformation methods are stochastic, our method samples a population of transformed images and performs the final classification on distributions of softmax probabilities. We train a separate compact distribution classifier to recognize distinctive features in the distributions of softmax probabilities of transformed clean images. Without retraining the original CNN, our distribution classifier improves the performance of transformation-based defenses on both clean and adversarial images, even though the distribution classifier was never trained on distributions obtained from the adversarial images. Our method is generic and can be integrated with existing transformation-based methods.

1 Introduction

There has been widespread use of convolutional neural networks (CNN) in many critical real-life applications such as facial recognition [18] and self-driving cars [8]. However, it has been found that CNNs are not robust to small perturbations to the input image. In other words, the CNN misclassifies

the input image when the image has been corrupted by an imperceptible change [23]. Such images are called adversarial examples and there has been much research in designing adversarial attacks that show the susceptibility of the CNN models. Correspondingly, many defense methods that aim to increase the CNN’s robustness to attacks have been proposed.

In this paper, we focus on transformation-based defenses where the input image is transformed in a certain way before feeding into the CNN, such that adversarial images will no longer be adversarial after the transformation. Existing transformation-based methods have shown considerable success in recovering from adversarial attacks. These methods are desirable because there is no need to retrain the CNN model and are thus model-agnostic. Furthermore, transformation-based defenses can be agnostic to the attack method. However, transformation-based defenses suffer from deterioration of performance on clean images. Figure 1 illustrates this tradeoff, where it shows the accuracies on the clean and adversarial images when we apply pixel deflection [19] on the CIFAR10 dataset. With increasing number of pixel deflections, there is recovery on the adversarial performance, but this comes with a rapid deterioration of performance on clean images.

We propose a defense mechanism that can be integrated with existing transformation-based defenses and reduce the deterioration of performance on clean images. Exploiting the fact that the transformation methods are stochastic, for each input image, our method samples a population of transformed images and performs the final classification on distributions of softmax probabilities. We train a separate compact distribution classifier to learn to associate the distinctive features of the distributions of softmax probabilities with the correct class label. If the individual transformed images were initially misclassified by the CNN, our distribution classifier should learn to recover the correct class.

Our method can be integrated as a plug-in with existing transformation-based defenses to enhance their performance. Note that our method has to be integrated with another robust defence method, it is not designed to be robust against attacks by itself. Through our experiments on the MNIST and CIFAR10 datasets on three defenses and four attacks, we show that our distribution classifier improves the classification accuracy on both clean and adversarial images, even though the distribution classifier was never trained on distributions obtained from adversarial images. On MNIST, the improvements in classification accuracy made by our distribution classifier are 1.7% and 5.9% on the clean and adversarial images respectively. On CIFAR10, the improvements are 6.4% and 3.6% respectively.

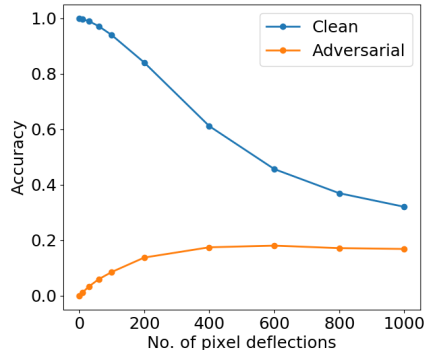


Figure 1: Pixel deflection defense [19] on CIFAR10: With increasing number of pixel deflections, there is recovery on the adversarial images but the performance on clean images deteriorates quickly.

2 Attacks and defenses

Given an image dataset $\{(x_1, y_1) \cdots (x_M, y_M)\}$ and a classifier F_θ that has been trained with this dataset, with parameters θ , the aim of the (untargeted) adversarial attack is to produce an adversarial image x_i^{adv} such that $F_\theta(x_i^{adv}) \neq y_i$ and $\|x_i^{adv} - x_i\|$ is small. In the case of a targeted attack, the adversary aims to change the prediction to the target class y_{target} : $F_\theta(x_i^{adv}) = y_{target}$.

There are a wide range of proposed adversarial attacks. In this paper, we focus on four attacks where the perturbation is computed for all image pixels. There are also attacks that perturb only a subset of the image pixels, for instance, one-pixel attacks [22] and adversarial patches [2]. We consider one single-step and three iterative attacks that have been used as benchmarks. In the following notations, we drop the subscript denoting the index of the data. Let $l(x, y; \theta)$ represent the differentiable cross entropy loss for the CNN classification.

Fast Gradient Sign Method (FGSM) [6]: This single-step attack simply uses the sign of the gradient of the classification loss function to perturb the image. The adversarial image is given by $x^{adv} = x + \epsilon \text{sign}(\nabla_x l(x, y; \theta))$, where ϵ controls the magnitude of the perturbation.

Iterative Gradient Sign Method (IGSM) [12]: IGSM is an iterative version of FGSM where at each iteration the pixel values are clipped to ensure that they are within the ϵ -neighborhood of the original image. The adversarial image is obtained with $x_0^{adv} = x$, and $x_{n+1}^{adv} = \text{clip}_{x,\epsilon} \{x_n^{adv} + \alpha \text{sign}(\nabla_x l(x_n^{adv}, y; \theta))\}$, where n represents the number of iterations and α is the step size per iteration.

DeepFool [16]: At each iteration, DeepFool approximates the classifier with a linear decision boundary and generates the minimal perturbation to cross the boundary. We use the L_2 norm for DeepFool.

Carlini & Wagner (C&W) [3]: The C&W L_2 attack jointly minimizes the perturbation L_2 norm and a differentiable loss function that is based on the classifier’s logit outputs.

$$\min_{x^{adv}} \left[\|x - x^{adv}\|_2^2 + c \max \left(Z(x^{adv})_y - \max \{Z(x^{adv})_k : k \neq y\}, -\kappa \right) \right], \quad (1)$$

where Z_k represents the classifier’s logit outputs for the k class. c controls the weightage given to the distortion cost and the classification cost and κ controls the confidence of the misclassification.

Defense methods have been proposed to make the classifiers more robust against attacks. In adversarial training, the CNN model is trained on adversarial examples generated from itself [15, 13] or from an ensemble of models [24]. In stochastic activation pruning (SAP) [5], during the test phase, a subset of activations in the network are randomly pruned while the remaining ones are scaled up to retain accuracy, and this randomness is found to give some robustness to adversarial attacks.

The above defense methods are model-specific as they require modification to the CNN. In the following, we introduce some model-agnostic methods. Pixel Defend [21] uses a generative PixelCNN to project input examples onto the data manifold before feeding them to the classifier. The idea is that the adversarial data will be ‘purified’ after projection. Defense-GAN [20] is based on a similar idea except that it uses a generative adversarial network. In the next section, we introduce another class of defense: input transformation defenses, where the input undergoes some transformation before feeding into the classifier. Transformation-based defense is the focus of our paper as it does not require retraining of the CNN and is agnostic to the attack method.

2.0.1 Transformation-based defenses

The aim of the input transformation defense methods is to maintain good accuracy on the clean images, that is, for input transformation T , $F_\theta(T(x_i)) = y_i$. The transformation has to also recover the images from adversarial perturbations: $F_\theta(T(x_i^{adv})) = y_i$. In many transformation-based methods, the transformation is stochastic, hence there can be different samples of the transformation of an image: $t_x \sim T(x)$, where t_x represents a transformed sample. Note that transformation-based defenses are implemented at test time, which is different from data augmentation which is implemented during training of the CNN. Here we introduce some state-of-the-art transformation-based methods.

Pixel deflection (PD) [19] : Pixel deflection corrupts an image by locally redistributing pixels. At each step, it selects a random pixel and replaces it with another randomly selected pixel in a local neighborhood. The probability of a pixel being selected is inversely proportional to the class activation map [27], and this protects regions that are important for classification from being corrupted. Lastly, there is a denoising step based on wavelet transform. In our experiments, we did not use robust activation maps. Instead, we randomly select pixels with equal probabilities. Our experiments show that this omission does not cause significant difference in performance.

Random resize and padding (RRP) [25] : Each image is first resized to a random size and then padded with zeroes to a fixed size in a random manner.

Quilting, total variance minimization (TVM) [7]: Image quilting constructs an image replacing patches of the original image with patches taken from a database. Guo et al. [7] also proposed total variance minimization (TVM) which constructs a substitute image that matches a randomly selected set of pixels in the original image, while having the lowest total variation.

Most image transformation defenses are stochastic and benefit from improved performance by taking the majority vote across samples of random transformations. The advantage of transformation-based methods is that there is no retraining of the CNN classifier which could be time-consuming. These methods are also flexible and work well across a range of classifier models and attacks.

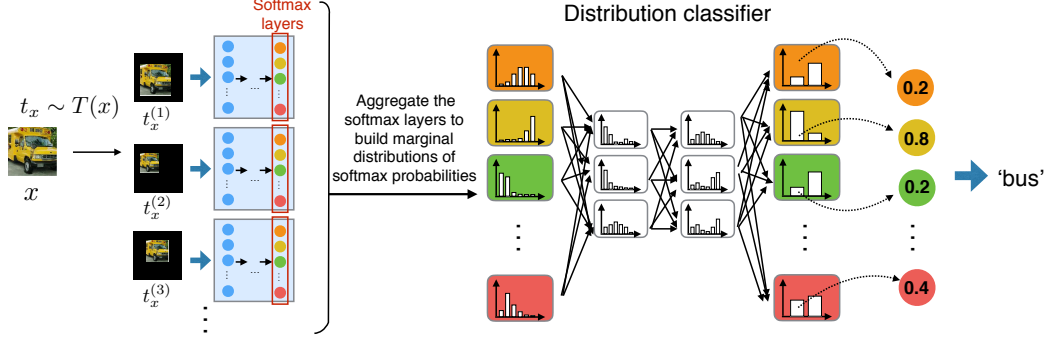


Figure 2: In transformation-based defenses, the image is transformed stochastically where each sample t_x is drawn from the distribution $T(x)$ and then fed to the CNN (blue box). In our defense method, for each input image x , we build the marginal distribution of softmax probabilities from the transformed samples $t_x^{(1)}, t_x^{(2)}, \dots$. The distributions are fed to a separate distribution classifier which performs the final classification.

However, a weakness of transformation-based methods, as identified by Prakash et al. [19], is that the transformation increases the accuracy on adversarial images at the expense of degrading the accuracy on clean images. In this paper, we target this shortcoming by proposing a defense method that improves the performance of transformation-based defenses on clean images.

3 Enhancing transformation-based defenses

Exploiting the fact that the transformation methods are stochastic, our method samples a population of transformed clean images and performs the final classification on distributions of softmax probabilities. To reduce the drop in performance on clean images, we train a separate compact distribution classifier to recognize patterns in the distributions of softmax probabilities of clean images. The details of the distribution classifier will be introduced in Section 3.1.

The steps below describe the training phase of our defense method, which is illustrated in Figure 2.

1. For each clean image x , obtain N transformed samples.
2. The transformed samples of the image $(t_x^{(1)}, t_x^{(2)}, \dots, t_x^{(N)})$ are fed into the CNN individually to obtain their softmax probabilities.
3. Step (2) generates a population of N softmax probabilities. We build the marginal distributions of the softmax from this population. We use kernel density estimation with a Gaussian kernel, followed by discretization of the distribution.
4. For each clean image x , the marginal distributions obtained in step (3) are signatures of x . We train our distribution classifier to learn to associate this signature with the correct class label. If the individual transformed images were initially misclassified by the CNN, our distribution classifier should learn to recover the correct class.

A formal description of our training method is given in the supplementary material. During the test phase, for any input image, clean or adversarial, we build the softmax distributions from N transformed samples and feed them into our trained distribution classifier to obtain the final prediction. Note that our defense method does not require retraining of the original CNN. Our method is also agnostic to the attack model and can be integrated with most existing transformation-based methods (see comparison in Table 1).

3.1 Distribution classifier

In our defense method, we use a distribution classifier which is trained on distributions of softmax probabilities obtained from transformed samples of the clean images. In doing so, our method boosts the accuracy on the transformed clean images. In this section, we describe our choice of distribution classifier. We adapt a state-of-the-art distribution-to-distribution regression method, called distribution

Table 1: Comparison of the range of defense techniques with our method. SAP: stochastic activation pruning, RRP: random resize and padding, TVM: total variance minimization.

Defense	Input transformation involved	Adversarial training of CNN	Modification to CNN network	Training of auxiliary network
Adversarial training [15]		Yes	Yes	No
Pixel Defend [21]	No	No	No	Yes
SAP [5]		No	Yes	No
Pixel deflection [19]				
RRP [25]	Yes	No	No	No
Quilting and TVM [7]				
Our method	Yes	No	No	Yes

Table 2: The attack models used for MNIST and CIFAR10, along with the distortion metrics and the success rates of the attacks. FGSM is the only single-step attack, hence its success rate is considerably lower than the other methods.

	MNIST (LeNet5)		CIFAR10 (Wide ResNet)	
	Distortion	Attack success rate (%)	Distortion	Attack success rate (%)
FGSM	$L_\infty = 0.39$	53.2	$L_\infty = 0.031$	58.2
IGSM	$L_\infty = 0.24$	91.2	$L_\infty = 0.24$	100.0
DeepFool	$L_2 = 0.06$	97.6	$L_2 = 0.042$	95.3
C&W	$L_2 = 0.142$	94.9	$L_2 = 0.023$	94.1

regression network (DRN) [10]. DRN encodes an entire distribution in each network node and this compact representation allows it to achieve higher prediction accuracies for the distribution regression task compared to conventional neural networks. Since DRN shows superior regression performance, we adapt DRN for distribution classification in this work.

Our adaption of the distribution classifier is shown on the right of Figure 2. The network consists of fully-connected layers, where each node encodes a distribution. The number of hidden layers and nodes per hidden layer is chosen by cross validation. The number of discretization bins for each distribution for the input layer and hidden layers are also tuned as hyperparameters. To adapt DRN for our distribution classification task, for the final layer, we have C nodes representing each class and we use 2 bins for each distribution to represent the logit output for the corresponding class. The cost function for the distribution classifier is the cross entropy loss on the logits. The distribution classifier is optimized by backpropagation using the Adam optimizer [9]. The weight initialization method follows Kou et al. [10], where the weights are sampled from a uniform random distribution.

4 Experiments

Datasets and CNN networks: We use the MNIST [14] and CIFAR10 [11] datasets. For the base CNN model for MNIST, we use the LeNet5 model [14] that has 98.7% test accuracy. For CIFAR10, we use the wide ResNet [26] with 95.7% test accuracy.

Attack methods: As introduced in Section 2, we use four commonly-used adversarial attacks in the untargeted setting. Table 2 shows the distortion metrics used and the attacks’ success rates of producing adversarial images for MNIST and CIFAR10. In the supplementary materials, we have included the hyperparameters used for each attack. For all attacks, the pixel intensities are clipped within the range $[0, 1]$. The attacks are implemented using the CleverHans library [17]. For L_2 norm, we use the root-mean-square distortion normalized by total number of pixels, following previous works. Out of the four attacks, FGSM is the only single-step attack, hence its success rate is considerably lower than the other methods.

Transformation-based defenses: As a baseline, we use a random pixel noise (RPN) transformation as a defense method, where each pixel noise is sampled with a uniform distribution with L_∞ measure. In addition, we use two state-of-the-art transformation-based methods: pixel deflection (PD) [19]

Table 3: MNIST results: For each attack, we compare the clean and adversarial (adv.) test accuracies with majority voting (Vote) and our distribution classifier method (DC). The three transformation-based defenses are random pixel noise (RPN), pixel deflection (PD) and random resize and padding (RRP). With no defense, the clean accuracy is 100% and the adversarial accuracy is 0%. Δ denotes the improvement of DC over voting. DC shows improvement over voting in most cases except when the initial voting performance was already very good.

		FGSM			IGSM			DeepFool			C&W		
		Vote (%)	DC (%)	Δ (%)	Vote (%)	DC (%)	Δ (%)	Vote (%)	DC (%)	Δ (%)	Vote (%)	DC (%)	Δ (%)
RPN	clean	95.4	97.8	+2.4	97.2	98.4	+1.2	100	99.9	-0.1	99.9	99.7	-0.2
	adv.	17.0	32.1	+15.1	77.9	90.9	+13.0	99.3	98.3	-1.0	99.7	99.5	-0.2
PD	clean	87.6	96.9	+9.3	98.9	98.8	-0.1	100	99.9	-0.1	99.0	99.4	+0.4
	adv.	17.1	22.6	+5.5	51.3	67.3	+16.0	99.4	99.4	0	93.8	98.0	+4.2
RRP	clean	91.4	98.2	+6.8	98.7	98.4	-0.3	98.9	99.1	+0.2	98.9	99.2	+0.3
	adv.	36.4	39.4	+3.0	71.1	82.4	+11.3	93.6	95.2	+1.6	95.3	97.4	+2.1

and image random resize and pad (RRP) [25]. Although these two methods have not been tested for MNIST and CIFAR10 in the previous works, we find that they work considerably well and present the results here. We implement the defense methods only on images which has been correctly predicted by the original CNN, following Prakash et al. [19]. The hyperparameter tuning for each defense method is conducted on the validation set for each dataset. We select hyperparameters that give the best recovery from adversarial attack, regardless of the deterioration in accuracy on clean images. The exact hyperparameters for the image transformation defenses for each dataset are included in the supplementary materials.

To test the effectiveness of the three transformation-based defenses before integrating with our defense method, we perform majority voting on the classification predictions of the transformed image samples. This sets the baseline for our distribution classifier defense method. When reporting the test accuracies, on clean images, we consider images that have been correctly predicted by the original CNN, hence without any defense method, the test accuracy is 100%. For adversarial images, we consider the images that have been successfully attacked, so the test accuracy reflects the recovery rate by the defense.

4.1 Implementation of our defense method

Our defense method uses a distribution classifier to train on distributions of softmax probabilities obtained from transformed samples of the clean images. For each image, we build the marginal distributions of the softmax for each class using kernel density estimation with a Gaussian kernel. The kernel width is optimized to be 0.05. For all layers except the final layer, the distribution discretization size is 100. For the final layer, the discretization step is 2, as explained in Section 3.1. The network architecture of the distribution classifier and optimization hyperparameters were chosen by cross-validation and are included in the supplementary material. After training on the distributions from clean images, the distribution classifier is tested on both clean and adversarial images.

4.2 MNIST results

For the MNIST dataset, $N = 100$ image transformation samples were used for voting and for constructing the distribution of softmax probabilities for each image. Kou et al. [10] showed that DRN has few parameters and requires few training data to generalize. We found that our distribution classifier required only 1000 training data, which is a small fraction out of the original 50,000 data. Table 3 shows the effectiveness of the three transformation-based defenses with majority voting and our distribution classifier. First, we observe that the recovery on adversarial images for the iterative methods IGSM, DeepFool and C&W is much better compared to the recovery for single-step FGSM. This is in line with the observations made by Xie et al. [25] where they found their transformation defense to be more effective for iterative attacks, since iterative attacks are more prone to overfitting to the CNN models.

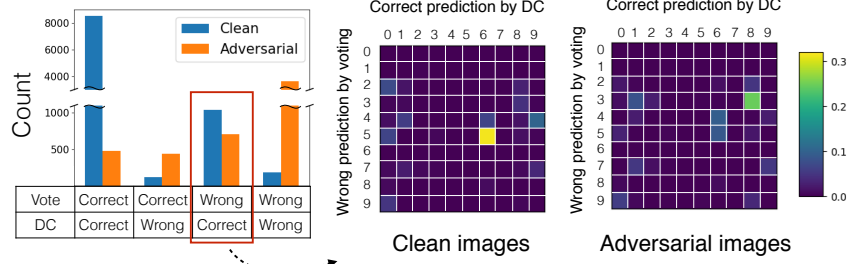


Figure 3: (Left) The breakdown of test prediction results by voting and our distribution classifier (DC) for clean and adversarial images. For both clean and adversarial images, DC performs better than voting as there are more data where voting predicts wrongly and DC predicts correctly (3rd column) than data where voting predicts correctly and DC predicts wrongly (2nd column). (Right) For data where voting predicts wrongly and DC predicts correctly, we obtain the breakdown across the MNIST classes where the heatmap represents percentage of data. We observe similarities between the heatmaps for clean and adversarial images which shows good transferability of improvement.

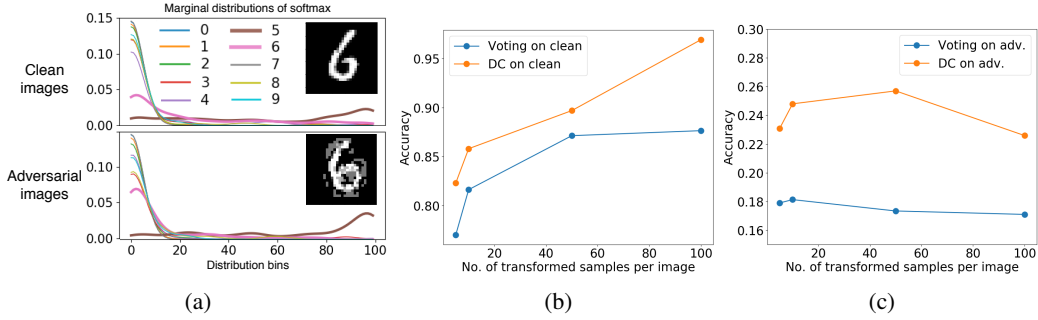


Figure 4: (a) Marginal distributions of the softmax probabilities for one example of clean image and one separate example of adversarial image where voting predicts class 5 (brown) wrongly but DC predicts class 6 (pink) correctly. Voting predicts class 5 as class 5's distribution peaks at higher softmax values, but DC learns more complex features from the distributions and corrects the prediction to class 6. (b) On the clean images, both voting and DC accuracies improves with more number of transformed samples. As number of samples increases, voting saturates while DC continues to improve. (c) On the adversarial images, the accuracies stay more or less the same as the number of transformed samples increases.

Our distribution classifier is trained to reduce the deterioration of performance on clean images. As Table 3 shows, our distribution classifier has improved accuracy over voting on the clean images for most cases, except when the initial accuracy was already high (eg. 100% to 99.9% for RPN and PD on DeepFool). For iterative DeepFool and C&W, the recovery rate by voting alone was already very high with little perturbation by RPN and PD. Since there was little or no deterioration of the accuracy on clean images, voting was already sufficient. On average, the improvement of the accuracy on the clean images is 1.7%. This shows that our distribution classifier is stronger than voting. Voting takes the mode of the softmax probabilities of each instance of the transformed image, disregarding properties such as entropy and variance across the classes. The final prediction is simply the class with the maximum vote. In contrast, our distribution classifier accumulates the softmax probabilities into the marginal distributions and learns from the distinctive features of the distributions.

Without training on the distributions obtained from adversarial images, our distribution classifier has managed to improve the recovery rate. This is observed for most cases, except when the recovery rate by voting was already high (eg. 99.7% to 99.5% for RPN on C&W). On average, the improvement of the accuracy on the adversarial images is 5.9%. Figure 3 shows the breakdown of the test prediction results. The dataset used was MNIST, attacked with FGSM and using PD defense. For both clean and adversarial images, DC performs better than voting as there are more data where voting predicts wrongly and DC predicts correctly (3rd column) than data where voting predicts correctly and DC predicts wrongly (2nd column).

Table 4: CIFAR10 results: For each attack, we compare the clean and adversarial (adv.) test accuracies with majority voting (Vote) and our distribution classifier method (DC). The three transformation-based defenses are random pixel noise (RPN), pixel deflection (PD) and random resize and padding (RRP). With no defense, the clean accuracy is 100% and the adversarial accuracy is 0%. Δ denotes the improvement of DC over voting. In all cases, there is improvement of DC over voting.

		FGSM			IGSM			DeepFool			C&W		
		Vote (%)	DC (%)	Δ (%)	Vote (%)	DC (%)	Δ (%)	Vote (%)	DC (%)	Δ (%)	Vote (%)	DC (%)	Δ (%)
RPN	clean	47.3	68.4	+21.1	47.3	66.8	+19.5	97.8	98.6	+0.8	95.8	97.5	+1.7
	adv.	16.9	24.8	+7.9	26.5	37.2	+10.7	91.4	93.0	+1.6	85.5	87.6	+2.1
PD	clean	75.9	84.1	+8.2	75.7	83.1	+7.4	93.5	94.6	+1.1	92.5	94.1	+1.6
	adv.	36.4	39.0	+2.6	51.7	58.2	+6.5	91.1	92.3	+1.2	88.5	90.8	+2.3
RRP	clean	81.9	88.4	+6.5	79.8	87.9	+8.1	97.6	97.7	+0.1	95.8	97.0	+1.2
	adv.	39.6	41.2	+1.6	56.0	61.3	+5.3	91.3	91.5	+0.2	87.7	89.3	+1.6

predicts wrongly (2nd column). We analyze the data that voting predicts wrongly and DC predicts correctly from the breakdown across the MNIST classes in the heatmaps, where the color represents the percentage of data. We observe similarities between the heatmaps for clean and adversarial images. For example, class 5 gets corrected to class 6, and class 3 gets corrected to class 8. This shows that the improvements made on the clean images are transferable to the adversarial images.

We further analyze why DC performs better than voting. Figure 4a shows the marginal distributions of the softmax probabilities for one example of clean and one example of adversarial image where voting predicts class 5 wrongly but DC predicts class 6 correctly. The mechanism of voting is straightforward: voting predicts class 5 because majority of the samples have high softmax values for class 5. However, DC learns more subtle and complex features from the distributions and associates such features to the correct class 6. Furthermore, DC is able to generalize and correct the class label for the adversarial image even though it is not trained on it.

4.2.1 Number of transformed samples required

We used $N=100$ transformed samples in our experiments. Hence, the evaluation time will be 100 times longer than if a single sample was used. Here we study the effect of the number of samples. Figure 4b and 4c show the classification accuracies for voting and DC as the number of transformed samples increases. On the clean images, both voting and DC accuracies improve with more number of samples, with the performance of voting saturating while DC’s performance continues to increase with widening gap. The widening gap shows that a sufficient number of samples is required to capture the features of the distribution of softmax probabilities. On the adversarial images, the accuracies stay more or less the same. Although having more transformed samples is beneficial for the performance on clean images, our distribution classifier improves the voting performance regardless of the number of samples.

4.3 CIFAR10 results

For the CIFAR10 dataset, $N = 50$ image transformation samples were used. We used 10,000 training data to train the distribution classifier. Table 4 shows the results for CIFAR10. Similar to the MNIST dataset, we saw the recovery on iterative attacks to be higher than the single-step FGSM. In all cases, we saw improvements for the distribution classifier over voting on both clean and adversarial images. On average, the improvement of the accuracies on the clean and adversarial images are 6.4% and 3.6% respectively. This shows that our distribution classifier is able to learn the distinctive features in the distributions of the softmax and outperforms voting.

5 Discussion

In this paper, we have introduced our distribution classifier method that can be integrated with transformation-based defenses to boost their performance on both clean and adversarial images. The

key idea behind our method is the transferability of improvement of performance from clean to adversarial images, allowing our distribution classifier to improve the performance on adversarial images without training on them. We improved the performance of transformation-based defenses on MNIST and CIFAR10. In future work, we will extend our method to datasets with more classes such as ImageNet [4]. Our method learns on the distribution of softmax probabilities from the transformed images. It is also interesting to consider distributions of the logits or intermediate layers. Our preliminary investigations show that using the distributions from the logits does not give significant improvement. Finally, Athalye et al. [1] have shown that under the white-box setting where the attacker has full knowledge of the CNN model and the defense, random transformation defenses are susceptible to further attack. Our distribution classifier is a differentiable network and there is a possibility our combined defense system can be subjected to further attack. In future work, we will study the end-to-end attack of our method. Note that susceptibility to end-to-end attacks of our method strongly depends on which image transformation the distribution classifier is integrated with. The distribution classifier alone is not designed to be robust against attacks.

References

- [1] Anish Athalye, Nicholas Carlini, and David Wagner. Obfuscated gradients give a false sense of security: Circumventing defenses to adversarial examples. *arXiv preprint arXiv:1802.00420*, 2018.
- [2] Tom B Brown, Dandelion Mané, Aurko Roy, Martín Abadi, and Justin Gilmer. Adversarial patch. *arXiv preprint arXiv:1712.09665*, 2017.
- [3] Nicholas Carlini and David Wagner. Towards evaluating the robustness of neural networks. In *2017 IEEE Symposium on Security and Privacy (SP)*, pages 39–57. IEEE, 2017.
- [4] Jia Deng, Wei Dong, Richard Socher, Li-Jia Li, Kai Li, and Li Fei-Fei. Imagenet: A large-scale hierarchical image database. In *2009 IEEE conference on computer vision and pattern recognition*, pages 248–255. Ieee, 2009.
- [5] Guneet S Dhillon, Kamyar Azizzadenesheli, Zachary C Lipton, Jeremy Bernstein, Jean Kossaifi, Aran Khanna, and Anima Anandkumar. Stochastic activation pruning for robust adversarial defense. *arXiv preprint arXiv:1803.01442*, 2018.
- [6] Ian J Goodfellow, Jonathon Shlens, and Christian Szegedy. Explaining and harnessing adversarial examples. *arXiv preprint arXiv:1412.6572*, 2014.
- [7] Chuan Guo, Mayank Rana, Moustapha Cisse, and Laurens van der Maaten. Countering adversarial images using input transformations. *arXiv preprint arXiv:1711.00117*, 2017.
- [8] Seokwoo Jung, Unghui Lee, Jiwon Jung, and David Hyunchul Shim. Real-time traffic sign recognition system with deep convolutional neural network. In *2016 13th International Conference on Ubiquitous Robots and Ambient Intelligence (URAI)*, pages 31–34. IEEE, 2016.
- [9] Diederik P Kingma and Jimmy Ba. Adam: A method for stochastic optimization. *arXiv preprint arXiv:1412.6980*, 2014.
- [10] Connie Khor Li Kou, Hwee Kuan Lee, and Teck Khim Ng. A compact network learning model for distribution regression. *Neural Networks*, 2018.
- [11] Alex Krizhevsky and Geoffrey Hinton. Learning multiple layers of features from tiny images. Technical report, Citeseer, 2009.
- [12] Alexey Kurakin, Ian Goodfellow, and Samy Bengio. Adversarial examples in the physical world. *arXiv preprint arXiv:1607.02533*, 2016.
- [13] Alexey Kurakin, Ian Goodfellow, and Samy Bengio. Adversarial machine learning at scale. *arXiv preprint arXiv:1611.01236*, 2016.
- [14] Yann LeCun, Léon Bottou, Yoshua Bengio, Patrick Haffner, et al. Gradient-based learning applied to document recognition. *Proceedings of the IEEE*, 86(11):2278–2324, 1998.

- [15] Aleksander Madry, Aleksandar Makelov, Ludwig Schmidt, Dimitris Tsipras, and Adrian Vladu. Towards deep learning models resistant to adversarial attacks. *arXiv preprint arXiv:1706.06083*, 2017.
- [16] Seyed-Mohsen Moosavi-Dezfooli, Alhussein Fawzi, and Pascal Frossard. Deepfool: a simple and accurate method to fool deep neural networks. In *Proceedings of the IEEE conference on computer vision and pattern recognition*, pages 2574–2582, 2016.
- [17] Nicolas Papernot, Fartash Faghri, Nicholas Carlini, Ian Goodfellow, Reuben Feinman, Alexey Kurakin, Cihang Xie, Yash Sharma, Tom Brown, Aurko Roy, Alexander Matyasko, Vahid Behzadan, Karen Hambardzumyan, Zhishuai Zhang, Yi-Lin Juang, Zhi Li, Ryan Sheatsley, Abhibhav Garg, Jonathan Uesato, Willi Gierke, Yinpeng Dong, David Berthelot, Paul Hendricks, Jonas Rauber, and Rujun Long. Technical report on the cleverhans v2.1.0 adversarial examples library. *arXiv preprint arXiv:1610.00768*, 2018.
- [18] Omkar M Parkhi, Andrea Vedaldi, Andrew Zisserman, et al. Deep face recognition. In *bmvc*, volume 1, page 6, 2015.
- [19] Aaditya Prakash, Nick Moran, Solomon Garber, Antonella DiLillo, and James Storer. Deflecting adversarial attacks with pixel deflection. In *Proceedings of the IEEE conference on computer vision and pattern recognition*, pages 8571–8580, 2018.
- [20] Pouya Samangouei, Maya Kabkab, and Rama Chellappa. Defense-gan: Protecting classifiers against adversarial attacks using generative models. *arXiv preprint arXiv:1805.06605*, 2018.
- [21] Yang Song, Taesup Kim, Sebastian Nowozin, Stefano Ermon, and Nate Kushman. Pixeldefend: Leveraging generative models to understand and defend against adversarial examples. *arXiv preprint arXiv:1710.10766*, 2017.
- [22] Jiawei Su, Danilo Vasconcellos Vargas, and Kouichi Sakurai. One pixel attack for fooling deep neural networks. *IEEE Transactions on Evolutionary Computation*, 2019.
- [23] Christian Szegedy, Wojciech Zaremba, Ilya Sutskever, Joan Bruna, Dumitru Erhan, Ian Goodfellow, and Rob Fergus. Intriguing properties of neural networks. *arXiv preprint arXiv:1312.6199*, 2013.
- [24] Florian Tramèr, Alexey Kurakin, Nicolas Papernot, Ian Goodfellow, Dan Boneh, and Patrick McDaniel. Ensemble adversarial training: Attacks and defenses. *arXiv preprint arXiv:1705.07204*, 2017.
- [25] Cihang Xie, Jianyu Wang, Zhishuai Zhang, Zhou Ren, and Alan Yuille. Mitigating adversarial effects through randomization. *arXiv preprint arXiv:1711.01991*, 2017.
- [26] Sergey Zagoruyko and Nikos Komodakis. Wide residual networks. *arXiv preprint arXiv:1605.07146*, 2016.
- [27] Bolei Zhou, Aditya Khosla, Agata Lapedriza, Aude Oliva, and Antonio Torralba. Learning deep features for discriminative localization. In *Proceedings of the IEEE conference on computer vision and pattern recognition*, pages 2921–2929, 2016.

A Formal description of our defense method

Here we give a formal description of our training method introduced in Section 3 of our main paper.

1. For each clean image x , obtain N transformed samples.
2. The transformed samples of the image $(t_x^{(1)}, t_x^{(2)}, \dots, t_x^{(N)})$ are fed into the CNN individually to obtain their softmax probabilities. Let $\sigma_x^{(i)}$ be the softmax vector derived from $t_x^{(i)}$, and $\sigma_{x,j}^{(i)}$, for $j = 1, \dots, C$, be the j -th component of the softmax vector. C denotes the number of classes for the classification task.
3. Step (2) generates a population of N softmax probabilities. We build the marginal distributions of the softmax from this population. We use kernel density estimation with a Gaussian kernel, followed by discretization of the distribution. Let $h_{x,j}$ be the distribution accumulated from $\sigma_{x,j}^{(1)}, \dots, \sigma_{x,j}^{(N)}$:

$$h_{x,j}(s) = \frac{1}{N\sqrt{2\pi}\delta} \sum_i^N \exp\left(-\frac{(s - \sigma_{x,j}^{(i)})^2}{2\delta^2}\right), \quad (2)$$

where δ is the kernel width.

4. We train the distribution classifier on the marginal distributions obtained in step (3). The marginal distributions $h_{x,1}(s), \dots, h_{x,C}(s)$ are C nodes that are fed into our distribution classifier, where the label is the ground truth class for image x . The distribution classifier is trained on the training set of clean images.
5. At test time, for any input image (clean or adversarial), we obtain the marginal distributions of the softmax probabilities following steps (1) to (3) and feed it to the distribution classifier to obtain the predicted class.

B Experimental setup

B.1 Adversarial attack hyperparameters

Table 5 shows the hyperparameter settings used for the adversarial attacks. The attacks are implemented using the CleverHans library [17]. For DeepFool and C&W, the other hyperparameters used are the default values set in CleverHans.

Table 5: Hyperparameter settings for the four adversarial attack methods.

	MNIST			CIFAR10		
	Distortion	Accuracy (%)	Settings	Distortion	Accuracy (%)	Settings
FGSM	$L_\infty = 0.39$	46.8	-	$L_\infty = 0.031$	41.8	-
IGSM	$L_\infty = 0.24$	8.8	100 steps, step size=0.004	$L_\infty = 0.24$	0.0	20 steps, step size=0.004
DeepFool	$L_2 = 0.06$	2.4	Max iter.=30	$L_2 = 0.042$	4.7	Max iter.=5
C&W	$L_2 = 0.142$	5.1	Max iter.=500	$L_2 = 0.023$	5.9	Max iter.=10

B.2 Image transformation defense parameters

Tables 6 and 7 show the image transformation parameters used for MNIST and CIFAR10 respectively. The hyperparameter tuning for each defense method is conducted on the validation set for each dataset. We select hyperparameters that give the best recovery from adversarial attack, regardless of the deterioration in accuracy on clean images.

Table 6: Details of the image transformation parameters for MNIST. The three transformation-based methods tested are random pixel noise (RPN), pixel deflection (PD) and random resize and padding (RRP). For RPN, the noise magnitude is unnormalized (out of 255). For PD, d is the number of deflections, w is the window size and σ is the denoising parameter.

	FGSM	IGSM	DeepFool	C&W
RPN	$L_\infty=130$	$L_\infty=90$	$L_\infty=10$	$L_\infty=10$
PD	d=300, w=20, $\sigma=0$	d=100, w=20, $\sigma=0$	d=10, w=20, $\sigma=0.08$	d=100, w=25, $\sigma=0.08$
RRP	resize range=[4,28]	resize range=[22,28]	resize range=[23,28]	resize range=[23,28]

Table 7: Details of the image transformation parameters for CIFAR10.

	FGSM	IGSM	DeepFool	C&W
RPN	$L_\infty=40$	$L_\infty=40$	$L_\infty=7$	$L_\infty=10$
PD	d=60, w=10, $\sigma=0.06$	d=80, w=10, $\sigma=0.06$	d=20, w=10, $\sigma=0.04$	d=80, w=10, $\sigma=0.04$
RRP	resize range=[20,25]	resize range=[19,25]	resize range=[28,32]	resize range=[23,32]

B.3 Distribution classifier network architecture

Our defense method uses a distribution classifier to train on distributions of softmax probabilities obtained from transformed samples of the clean images. For each image, we build the marginal distributions of the softmax for each class using kernel density estimation with a Gaussian kernel. The kernel width is optimized to be 0.05. For all layers except the final layer, the distribution discretization size is set at 100. For the final layer distributions, the discretization step is set at 2, as explained in our main paper. The network architecture of the distribution classifier and optimization hyperparameters were chosen by cross-validation.

Table 8: Network architecture for the distribution classifier for MNIST, where 2x10 represents 2 hidden layers of 10 nodes.

	FGSM	IGSM	DeepFool	C&W
RPN	1x10	2x10	1x10	1x10
PD	1x10	1x10	1x20	1x20
RRP	1x10	1x10	1x20	1x20

Table 9: Network architecture for the distribution classifier for CIFAR10, where 2x10 represents 2 hidden layers of 10 nodes.

	FGSM	IGSM	DeepFool	C&W
RPN	1x10	1x20	1x20	1x20
PD	1x20	1x10	1x20	1x10
RRP	1x20	1x10	1x20	1x10